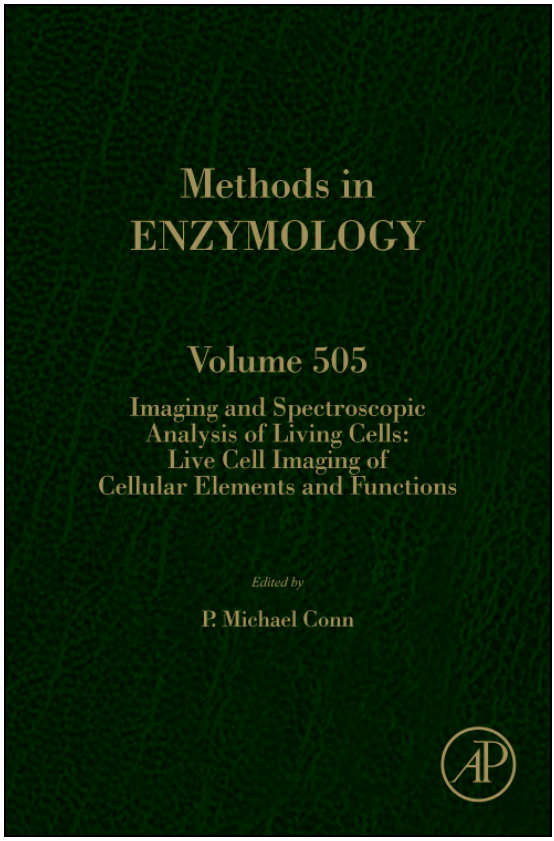

From: Moira J. Sheehan and Wojciech P. Pawlowski, Imaging Chromosome Dynamics in Meiosis in Plants. In P. Michael Conn, editor: Methods in Enzymology, Vol. 505, Burlington: Academic Press, 2012, pp. 125-143.
ISBN: 978-0-12-388448-0

CHAPTER SEVEN

Imaging Chromosome Dynamics in Meiosis in Plants

Moira J. Sheehan* *and* Wojciech P. Pawlowski†

Contents

Abstract

Progression of meiosis has been traditionally reconstructed from microscopic images collected from fixed cells. This approach has clear shortcomings in accurately portraying the dynamics of meiotic processes. Studies conducted in recent years mostly in unicellular fungi have shown that chromosomes in meiotic prophase exhibit dynamic motility that cannot be accurately examined using fixed cell imaging. However, in contrast to yeast, research on meiotic chromosome dynamics in multicellular eukaryotes has been lagging. This was in part because meiocytes in multicellular eukaryotes reside deep within reproductive organs and are often refractory to culturing. Here, we describe a method in which intact, live-plant reproductive organs (anthers) are cultured to enable

* Nature Source Genetics, Ithaca, New York, USA
† Department of Plant Breeding and Genetics, Cornell University, Ithaca, New York, USA

Methods in Enzymology, Volume 505
ISSN 0076-6879, DOI: 10.1016/B978-0-12-388448-0.00015-2

monitoring chromosome dynamics of meiocytes using multiphoton excitation (MPE) microscopy. The method was developed for use in maize but can be applied to other plant species and adapted for use in other taxa in which meiocytes are embedded in multicellular reproductive structures. MPE microscopy allows visualization of meiocytes embedded within native tissue *in planta* and thus meiocytes remain intact for the entire imaging procedure. We detail the kinds of time-lapse movies that can be captured and analyzed using this technique and also highlight software packages that can be utilized for analysis of movies chromosome dynamic in live meiocytes.

1. Introduction

Meiosis is a specialized type of cell division that leads to the production of gametes in the vast majority of plants, animals, and fungi. It consists of two consecutive divisions, meiosis I and meiosis II, that take place without an intervening S phase. During meiosis I, homologous chromosomes, one from each parent, find each other, pair, and recombine to form bivalents. Subsequently, a haploid set of chromosomes segregates to each daughter cell. In contrast to meiosis I, meiosis II is similar to a typical mitosis. The longest and most complex stage of meiosis is prophase of meiosis I (Fig. 7.1). Dramatic changes in chromosome behavior and morphology during meiotic prophase I are used to subdivide it into five stages (Zickler and Kleckner, 1999). In leptotene, decondensed chromatin becomes organized into chromosomes by the assembly of a proteinaceous chromosome core. In zygotene, homologous chromosomes pair. Pairing is followed by synapsis, when the central element of the synaptonemal complex (SC) is installed between the paired homologous chromosomes and stabilizes the pairing interaction (Page and Hawley, 2004). In pachytene, fully paired and synapsed chromosomes are visible as bivalents. In diplotene, the SC disassembles and chiasmata, which hold homologs together, are visible. Finally, in diakinesis, the chromosomes undergo the final stage of condensation.

During early stages of meiotic prophase, chromosomes undergo major spatial reorganization, which includes their repositioning in the nucleus. In most eukaryotes, the chromosome repositioning includes clustering of telomeres on the nuclear envelope during zygotene, a process known as the telomere bouquet formation (Harper *et al.*, 2004; Scherthan, 2007). While telomeres cluster, centromeres generally point the other direction, resulting in a telomere–centromere polarization of the meiocyte nucleus (Cowan *et al.*, 2001). The chromosome arrangement formed as a result of the bouquet formation is thought to reduce the spatial separation and misalignment of homologous loci within the nucleus before homologous chromosomes identify each other and pair.

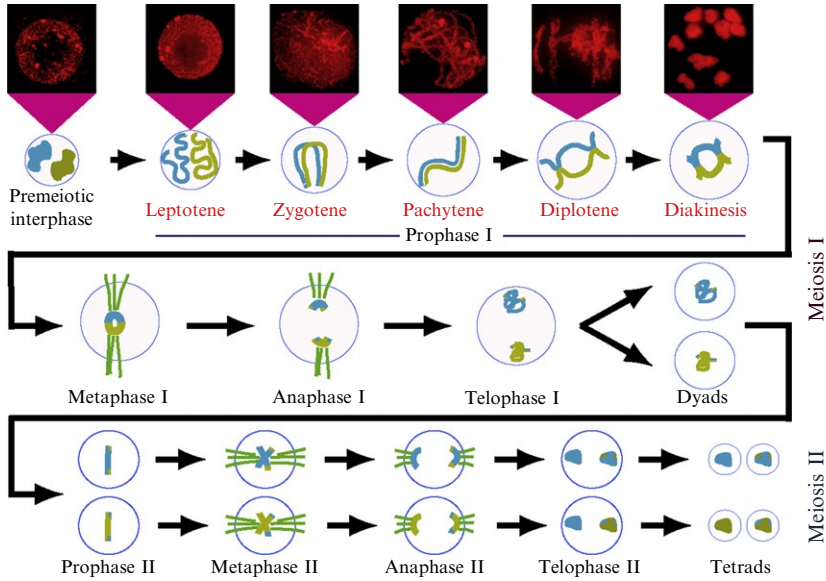

Figure 7.1 An overview of meiosis. Only one pair of chromosomes is shown. Each chromosome is of different color. Images on the top show chromosomes in maize male meiocytes stained with DAPI. The images are flat projections of 3D image stacks collected using 3D deconvolution microscopy.

Reconstructions of the progression of meiotic prophase have been traditionally conducted using fixed meiocytes. Although these reconstructions provided information on the general patterns of chromosome behavior, live imaging studies conducted in a number of species (Baudrimont *et al.*, 2010; Chikashige *et al.*, 1994; Conrad *et al.*, 2008; Koszul *et al.*, 2008; Sheehan and Pawlowski, 2009) showed that observations of fixed cells are not able to convey the dynamics and complexity of chromosome behavior in live meiocytes. Live microscopy of chromosome dynamics during meiotic prophase I was first conducted in budding and fission yeasts. These studies revealed that zygotene and pachytene are periods of very dynamic chromosome motility, which is closely associated with transient deformation of the nuclei (Chikashige *et al.*, 1994; Scherthan *et al.*, 2007; Trelles-Sticken *et al.*, 2005). In fission yeast, nuclear movements are particularly dramatic and known as horsetail movements, in which the entire nucleus violently moves back and forth (Chikashige *et al.*, 1994). Interestingly, while in fission yeast motility of all chromosomes is highly coordinated, in budding yeast, chromosomes move independently from each other (Scherthan *et al.*, 2007; Trelles-Sticken *et al.*, 2005).

Methods for observations of live cells undergoing early stages of meiosis have been also recently developed in multicellular eukaryotes. We describe here a live imaging technique that we devised to examine chromosome dynamics in meiotic prophase I in male meiocytes of maize (Sheehan and Pawlowski, 2009). This method can also be used in other plant species and could be adapted for use in other taxa in which meiocytes are embedded in multicellular reproductive structures. Using this technique, we found that meiotic chromosomes in maize exhibit, similarly to yeast, extremely vigorous motility. We discovered that the chromosome movements are stage specific and more complex than the movements observed in yeast. In zygotene, small chromosome regions, mostly chromosome ends, exhibit short-range movements. In pachytene, these fast movements are replaced by slower, sweeping motions of large chromosome segments. In addition to the motility of individual chromosome segments, the entire chromatin in the nucleus is subject to oscillating rotational motions. The rotational movements persist through zygotene as well as pachytene.

2. Technical Considerations

2.1. Using multiphoton excitation (MPE) microscopy for imaging meiocytes inside reproductive structures

Meiocytes in higher plants are embedded in multicellular reproductive structures and are difficult targets for live imaging. Although isolated plant meiocytes at the metaphase I and anaphase I stages can be cultured and imaged with standard wide-field microscopy techniques (Yu *et al.*, 1997), attempts to culture isolated meiocytes at the prophase I stage of meiosis proved unsuccessful (Chan and Cande, 2000; Heslop-Harrison, 1966). The system we describe here relies on imaging meiocytes inside intact anthers (male reproductive organs), which in contrast to isolated meiocytes, can be cultured over the duration of meiosis (Cowan and Cande, 2002). In this approach, meiocytes are left undisturbed in their native environment, which facilitates their long-term viability.

Plant meiocytes develop in the center of the anther locule, which in maize during prophase I lies roughly 70–100 μ from the anther surface (Fig. 7.2). This depth is beyond the capabilities of confocal microscopy. It is, however, within the demonstrated range of $\sim$200 μ of multiphoton excitation (MPE) microscopy (Denk *et al.*, 1990). In addition to its deeper imaging capabilities, MPE microscopy has other advantages that make it ideally suited for live imaging of plant tissues. It allows for excitation of fluorophores at lower energies using subpicosecond pulses of light, which are confined to a subfemtoliter focal volume, reducing signal-to-noise ratio (Denk *et al.*, 1990; Feijo and Cox, 2001; Williams *et al.*, 2001). This feature allows also

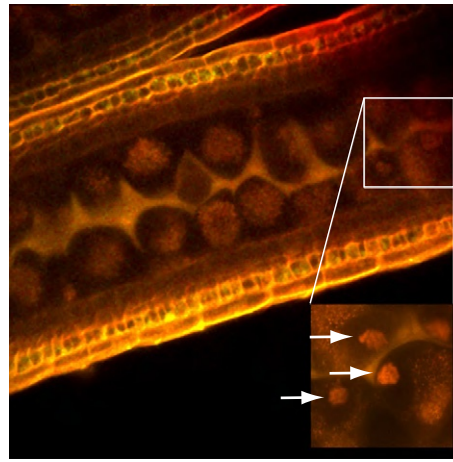

Figure 7.2 An optical cross section through a living maize anther generated with MPE microscopy. The anther was stained with DAPI (pseudocolored red) and MitoTracker Green FM (green). A fragment of the anther locule is magnified in inset. Arrows point to three meiocyte nuclei at the zygotene stage.

for high-resolution imaging of opaque tissues and reduces photobleaching, since fluorophores outside of the focal volume are not excited.

2.2. Culture medium

The purpose of culture medium in conventional tissue culture techniques is to encourage tissue growth. Consequently, the medium is usually supplemented with growth regulators and sugar as an easily accessible energy source. In contrast, culturing organs for live imaging requires isotonic solutions to maintain tissue viability without altering the speed of growth and development. Further, the medium should be close to optically clear to reduce light scattering.

To image meiosis in cultured excised anthers, we use artificial pond water (APW; Miller and Gow, 1989), which is an optically clear isotonic medium. We also tested Murashige and Skoog (MS) medium (which contains sucrose, i-inositol, inorganic salts, and vitamins: glycine, nicotinic acid, myo-inositol, pyridoxine, and thiamine). MS is the most commonly used plant tissue culture medium. However, we found that it had inferior optical clarity compared to APW. Additionally, as APW is a minimal medium (i.e., lacks a carbon source), it is less likely than MS medium to become contaminated by bacteria over the course of experiments. To maintain normal anther growth rate, APW is not supplemented with any growth regulators. Although APW should not be used for long-term

culturing (several days or longer), we found that anthers had excellent viability for over 30 h, as evidenced by mitochondrial viability staining (Emaus *et al.*, 1986; Johnson *et al.*, 1980; Keij *et al.*, 2000). For example, we observed zygotene meiocytes that progressed to pachytene and pachytene cells that progressed to dyads. Both progression patterns were consistent with the timing of meiosis observed *in planta* (Hsu *et al.*, 1988).

2.3. Chromosome staining

A good live imaging stain should effectively penetrate the tissue and not alter chromosome dynamics patterns. Stains used for fixed tissues are often also appropriate for live imaging, although live tissues are generally more difficult to stain and may require higher stain concentrations. For MPE microscopy, an additional consideration is the fluorophore emission wavelength. Stains with emission in blue or green are the easiest to use in MPE. Stains with yellow and red emissions may also be used but require an MPE system with a laser that can be tuned to an excitation wavelength of 900–950 nm. A range of stains with different color emissions are available for MPE (Table 7.1). These stains can be excited at the same fixed wavelength of 800 nm, allowing several stains to be used in a single experiment.

We use 4′,6-diamidino-2-phenylindole (DAPI) to visualize chromosomes. We found that DAPI provides an excellent vital stain for DNA in our anther culture system and requires shorter incubation times than other dyes we tested. In addition, DAPI was also more resistant to photobleaching than the other dyes, allowing us to take a larger number of exposures or more frequent exposures. DAPI stains entire chromosomes, although it does show some preference for heterochromatin. In particular, it intensely stains the heterochromatic knobs of maize, a feature that we found helpful for monitoring chromosome movements, as it provided fixed locations on chromosomes that we could follow when analyzing live imaging movies.

Table 7.1 Summary of cellular stains that can be used for live imaging studies with MPE

Emitted light	Fluorophore	Application
Blue	Hoechst 33342	Chromatin stain
	DAPI	Chromatin stain
Green	SYBR green	Nucleotide stain
Orange/yellow	Ethidium homodimer	Nucleotide stain
Red	Rhodamine 123	Mitochondrion stain
	Propidium iodide	Plant cell walls, nucleotide stain

These fluorophores can all be excited with a single wavelength of 800 nm but emit light at different wavelengths. The stains are available from Molecular Probes (Eugene, USA).

We also tested several other vital chromatin stains. SYTO-12 (Molecular Probes, Invitrogen, Carlsbad, CA) was previously reported to stain DNA in isolated live maize meiocytes at metaphase I (Chan and Cande, 2000; Yu *et al.*, 1997). However, we found that it did not adequately penetrate the intact anthers in our live imaging method. Several other SYTO stains with published reports of plant DNA staining, including SYTO 11, SYTO 13, SYTO 14, SYTO 15, and SYTO 16, also did not produce adequate staining, either due to penetration problems or rapid photobleaching. It is possible that incubation times longer than what we tested (1 h) would improve efficacy of these stains.

To aid stain penetration of the anther tissue, we add dimethyl sulfoxide (DMSO) to the anther culture medium at a final concentration of 1%. DMSO is known to polymerize microtubules *in vitro*. However, it does so when used at concentrations between 8% and 12% (Paleček and Hašek, 1984; Xu *et al.*, 2005), which are much higher than the concentrations that we used. Consistently, we did not see any difference in either chromosome or cytoplasmic (organellar) motility between DMSO concentrations ranging from 0.1% (which is frequently used in live confocal microscopy experiments; DeBolt *et al.*, 2007) to 5%.

2.4. Meiocyte viability

In live imaging system, there is a need to monitor cell viability in order to distinguish dead cells from cells whose dynamics are disrupted for other reasons. We chose to visualize mitochondrial activity as a way of monitoring cell viability because many live mitochondrial stains are available and could be tried. We tested three dyes that can only fluoresce when within actively respiring mitochondria. We found that Rhodamine 123, used at a final concentration of 20 μM, provides the most consistent mitochondrial staining of meiocytes of the three stains. $DiOC_7(3)$, which was previously reported to stain mitochondria in plants (Liu *et al.*, 1987), was tested by us at a final concentration of 200 μM. Although we could detect $DiOC_7(3)$ staining in anther epidermal layers, it was not visible in meiocytes, suggesting that the stain could not sufficiently penetrate to the inside of the anther. MitoTracker Green FM was tested at a final concentration of 200 nM. It provided sufficient mitochrondrial staining in leptotene meiocytes but staining was not reliably found in zygotene or pachytene meiocytes.

2.5. Cytoskeleton-disrupting drugs

Our anther imaging system allows for easy delivery of drugs to test their effect on chromosome dynamics. We tried two cytoskeleton-disrupting drugs: latrunculin B (Lat B), which disrupts the actin microfilament cytoskeleton, and colchicine, which disrupts the microtubule cytoskeleton.

Lat B was tested at final concentrations of 300 n*M*, 500 n*M*, and 1 μM. These concentrations were at or above the concentrations used in previous studies in plants (Baluska *et al.*, 2001; Chen *et al.*, 2007; Gibbon *et al.*, 1999). Colchicine was used at final concentrations of 100 μM, 1 m*M*, and 5 m*M* (Cowan and Cande, 2002). The drugs were administered together with DAPI. A 1 h incubation was allowed, regardless of drug concentration. After that, the drug/stain solution was removed and replaced with APW without DAPI but with the same drug concentration. This treatment removed unincorporated DAPI while maintaining a constant concentration of the drug throughout the imaging period.

2.6. Post-image collection data analysis

Analysis of images collected from living cells is often difficult, particularly when it comes to multidimensional movies: 4D (multiple optical sections through a 3D object over multiple time points) and 5D (multiple optical sections with multiple wavelengths through a 3D object over multiple time points). There are several software packages that can assist with image analysis and curation. We briefly describe here two proprietary packages, Imaris and Volocity, but focus on a freeware package, ImageJ, that we use exclusively in our chromosome movement image analyses.

2.6.1. Imaris by Bitplane

Imaris was originally released in 1993 to assist with confocal 3D image analyses. Today, it functions as a visualization and interpretation package for Windows. It can handle very large 3D and multiwavelength 3D images collected using most confocal microscopy systems as well as most wide-field microscopes. Imaris also has deconvolution algorithms to improve signal-to-noise ratio of the images. Users can automatically or manually select objects based on their size, shape, or brightness, and calculate key statistics of these objects using the MeasurementPro module. The automated selection function can make patterns that could be overlooked with manual assessment more obvious. Another outstanding feature of Imaris is the choice of five volume-rendering algorithms, allowing production of sophisticated 3D and 4D images and movies. Volumes and surfaces can be calibrated with overlaid objects. Even with all these computationally intensive applications, multithreaded processing makes Imaris run quickly and efficiently. Lastly, the Imaris suite, along with its volume-rendering and video applications, produces publication-quality documentation. First-time users, however, may find the breadth of functionality of this software package overwhelming. Like most packages, Imaris cannot handle 5D movies.

2.6.2. Volocity by PerkinElmer

Volocity is a start-to-finish package allowing everything from image acquisition to 3D rendering of analyzed images. Like Imaris, Volocity was designed to analyze images from confocal microscopy systems in 3D and in 3D with multiple wavelengths. The acquisition software is 64-bit based (providing more memory allocation and faster data processing than the traditional 32-bit systems), which lets the software capture large images more easily, significantly improving image capture speed and allowing higher image resolution. Wide-field fluorescence images can be "restored" with algorithms that remove out-of-focus haze, improving images to confocal-like quality. Like Imaris, Volocity has a number of algorithms for volume rendering of 3D and multiwavelength images. It also offers the ability to find, measure, and track objects in 2D, 3D, and 4D. With object tracking, the velocity, direction, distance traveled, and the path from start-to-finish are recorded and can be used to generate image overlays of object movement. Volocity can easily track hundreds of objects. There are also capabilities within the software package for analyzing colocalization, FRET, FRAP, and 3D ratio images. Volocity cannot handle 5D movies.

2.6.3. ImageJ by NIH

ImageJ is a Java-based program with a large community of developers and many resources. It offers a number of advantages over other image-analysis software, including the availability and ease of use of custom-designed plugins for many different types of image analyses. However, ImageJ only functions as an analysis package and cannot do image acquisition. ImageJ can be used for almost any image-analysis applications, including agarose gel documentation, photographic analysis, aerial photography analysis, microscopy, medical imaging, etc. Objects can be selected, measured for a number of parameters, and the data can be exported to a spreadsheet file. Objects can be traced through 3D space and tracked through time. However, both of these functions are not automatic but require manual input. Velocity, direction, distance, and path traveled are determined for every object tracked, and track overlays can easily be made for images. ImageJ can make movies (in the QuickTime and AVI formats) both flat and in 3D. There are several plugins designed for 3D, 4D, and 5D image analysis, but the effectiveness of the 4D and 5D analyses methods vary depending on the type of images collected. There are no volume-rendering plugins currently available.

A user with no previous image-analysis experience will feel comfortable with ImageJ and will be able to get it running quickly with the basic built-in functions. A more advanced user may seek additional plugins for more complex image manipulations. We exclusively used ImageJ for our live image analyses, to track moving objects, straighten chromosomes, calculate

rotational rocking movements, monitor nuclear envelope deformation, measure area in 2D, and generate movies with and without object-tracking overlays.

3. Protocols and Methods

3.1. Preparation of plant materials

To ensure availability of anthers at desired meiosis stages, plants for live imaging should be grown in a growth chamber or greenhouse at regular intervals. The time from planting to meiosis varies by genotype and is affected by environmental conditions. In maize, all anthers on the plant usually enter meiosis within less than a week of each other. To ensure uninterrupted availability of anthers, 5–10 seeds should be sown every week.

3.2. Anther staging and dissection

In maize and other grasses, immature flowers that contain cells undergoing meiosis are not visible without dissection. A determination of meiotic stage is, therefore, required prior to flower harvesting. For most meiosis studies in maize, male flowers are used because (1) the developmental timing of male meiocytes in maize is synchronized within anthers and florets and is less variable, (2) there are many more male meiocytes than female meiocytes on a plant, and (3) dissection of male flowers is much easier than female flowers and carries less potential for damage to the meiocytes.

Determining the developmental stage of male meiocytes in maize is not difficult but requires some practice. To stage and harvest flowers for live imaging of meiosis, we use the following protocol:

1. We usually determine the stage of meiosis before harvesting the tassel. At the time of meiosis, the immature tassel (the male inflorescence) is still inside the stalk. The presence of the tassel can be felt just below the top node of the plant by gently squeezing the leaf whorl.
2. When we establish that the tassel is large enough to be felt at the first node, a small incision is made with a razor blade through the leaves to the tassel, just below the top node.
3. For staging, several florets are removed with needle-nosed forceps into a glass scintillation vial containing 3:1 ethanol: acetic acid fixative.
4. The collected flowers are dissected on a microscope slide under a stereo dissecting microscope.
5. A drop of acetocarmine solution is added to the anthers for staining. Anthers are mixed with the stain using a dissecting needle over gentle heat until the color of the stain turns from deep red to purple. A cover

slip is placed over the anthers and gently pressed on to break the anthers and release meiocytes. The stage of meiosis is determined under a wide-field light microscope (as described by Golubovskaya *et al.*, 2002).

6. If the anthers are not yet at the desired meiosis stage, the incision is taped over with masking tape and the staging procedure is repeated in a day or two.
7. Plants with tassels containing anthers at the desired stage of meiosis are harvested at several nodes below the tassel and taken to the laboratory for anther dissection.
8. Leaves surrounding the tassel are gently removed. To prevent the tassel from drying out, the tassel is placed on wet paper towels in a tray and more wet paper towels are placed on top of the tassel.

Required reagents

- Fixative: a 3:1 mixture of 100% ethanol and glacial acetic acid.
- Acetocarmine: to stain chromosomes for the determination of meiosis stage.
  - Dissolve 2% acetocarmine powder in 45% acetic acid.
  - Boil 6–8 h in a flask with an attached reflux column.
  - Filter through paper filter when the solution is still warm. Keep in dark.

Required materials

- Needle-nosed forceps
- Dissecting needles
- Razor blades or scalpels
- Glass scintillation vials
- Glass microscope slides and cover slips
- Dissecting stereo microscope
- Wide-field light microscope

3.3. Collecting anthers for live imaging

After locating florets that contain anthers at the desired stage of meiosis, several anthers are collected for live imaging. In maize, each floret has three large anthers, which develop synchronously. All three anthers may be dissected. We always use two of the three anthers for live imaging. For example, one anther can be used for a drug treatment, while the other one can be used as a control. We found that precise meiosis stage determination is more difficult in live anthers than in fixed anthers. Therefore, the third anther from each floret is placed in a paraformaldehyde fixative for more accurate staging.

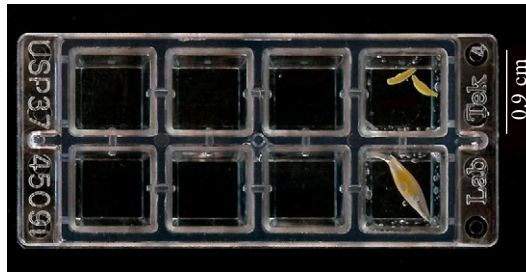

Figure 7.3 The 8-chamber culture slide used for live imaging of maize anthers. The chamber on the upper right contains two maize anthers. The chamber on the lower right contains an entire maize floret.

During dissection, care must be taken to not puncture or damage the anther, as it may cause the meiocytes to die. The dissected anthers are placed in a microscope chamber slide containing ~200 μl of anther culture medium (Fig. 7.3). Anthers are stained with a solution of DAPI in the anther culture medium for 1 h to allow good stain penetration of the inside of the anther. After the incubation, the stain solution is replaced with DAPI-free anther culture buffer. The chamber slide should be protected from light whenever possible to minimize photobleaching of fluorophores. Imaging can begin immediately.

Required reagents

Several reagents must be prepared in advance of collecting anthers for live imaging experiments.

- APW: the anther culture medium. Contains 0.1 *M* NaCl, 0.1 *M* $CaCl_2$, and 0.1 *M* KCl, mixed, filter-sterilized, and stored at room temperature.
- DAPI solution: chromatin stain. Make a concentrated stock of 50 mg ml^{-1} in water. Add to APW on day of anther harvest for a final concentration of 50 μg ml^{-1}. Store stock at −20 °C.
- DMSO: added to enhance penetration of stains and other reagents through anther tissues. Use at final concentration of 1% for DAPI staining but no more than 5% for any other application. Store stock at −20 °C. Add to APW on the day of anther harvest.
- Rhodamine 123: mitochondrial activity stain used to monitor cell viability. Rhodamine 123 (Invitrogen, Carlsbad, CA) will generate green fluorescence in actively respiring mitochondria. Make a stock solution of 20 m*M* in DMSO, store at −20 °C. Use at a final concentration of 20 μ*M*.
- Paraformaldehyde fixative: this fixative preserves the chromatin and chromosome structures better than the ethanol: acetic acid fixative and is used by us for precise determination of the meiosis stage in the third

anther of each floret from which anthers are collected for live imaging. Contains Buffer A (Bass *et al.*, 1997), 4% electron microscopy-grade paraformaldehyde, 50 μg ml^{-1} DAPI, and 1% DMSO. To fix anthers, incubate them in the fixative for 1 h with gentle shacking. After the incubation, replace with buffer A and wash the anthers for 1 h.

Buffer A recipe

- 20% of 10× buffer A salts (150 m*M* PIPES, 800 m*M* KCl, 200 m*M* NaCl, 20 m*M* Ethylenediaminetetraacetic acid (EDTA), 5 m*M* ethylene glycol tetraacetic acid (EGTA) in water, pH with 1 *M* NaOH to 6.8, store at 4 °C)
- 0.1% spermine stock (0.4 *M* spermine tetra HCl (Sigma S-2876) in 50 m*M* PIPES, store at −20 °C)
- 0.25% spermidine stock (0.4 *M* spermidine (Calbiochem 56766)) in 50 m*M* PIPES, store at −20 °C
- 0.2% DTT stock (1.0 *M* dithiothreitol (Calbiochem 233155)) in 0.01 *M* sodium acetate, pH 5.2, store at −20 °C
- 32% sorbitol stock (2 *M* solution in water, store at 4 °C).
- water

Filter-sterilize and store at 4 °C.

Optional reagents

The anther culturing system can be easily used to test the effects of various drugs on meiocyte development and chromosome dynamics. Drugs are added to the DAPI-containing anther culture medium for incubation simultaneous with chromosome staining. After staining, the culture medium should be replaced with medium free of DAPI but with the same concentration of the drug. We used this approach to test the effects of cytoskeleton-disrupting drugs:

- Lat B: disrupts actin filament polymerization. 100 μ*M* Lat B (Sigma-Aldrich, St. Louis, MO) stock solution should be stored at −20 °C. We used final concentrations of 500 n*M* and 1 μ*M*.
- Colchicine: disrupts microtubule polymerization. 100 m*M* colchicine (Sigma-Aldrich, St. Louis, MO) stock solution should be stored at −20 °C. We used final concentrations of 1 m*M* and 5 m*M*. For the 1 m*M* colchicine concentration, we used DMSO at a final concentration of 1% but for the 5 m*M* colchicine treatment, we used 5% as the final DMSO concentration.

Required materials

- Culture chamber microscope slides, sterile. We use the 8-chamber culture slides (Fig. 7.3; Nunc-155411, Thermo Fisher Scientific, Rochester, NY).

One to two anthers can be placed in each chamber filled with ~200 μl of culture medium (Fig. 7.3). Chamber slides are also available with a single chamber, 2-, 4- and, 16-chambers. Prior to anther collection, the chambers should be prefilled with the desired culture medium.

- Disposable transfer pipettes, fine-tipped: useful for applying and removing washes and other solutions to and from the culture chamber. Some examples of the pipettes are models 70960–3, -4, and −5 available at http://www.emsdiasum.com/microscopy/products/preparation/pipette.aspx.
- Adjustable volume micropipettes: used for mixing culture medium components.

3.4. MPE image capture

The exact MPE settings and acquisition method will vary depending on the microscope workstation used. In our MPE system, we use a TI:Sapphire laser tuned to 780–800 nm to detect both DAPI and Rhodamine 123. For imaging, the microchamber slide should be firmly placed on the microscope stage with clips, and the chamber lid should be left on, to minimize dust contamination. Prior to imaging, it may be useful to first locate the anthers inside the culture chamber using the eyepieces rather than the image acquisition software.

MPE images can be collected at one or more optical sections through the 3D object using one or more wavelengths. 2D images taken at a single *Z*-section and at a single time point are useful for measuring objects (lengths, areas, diameters, etc.) and for acquiring wide views of tissue structures (see Fig. 7.2). To capture and analyze chromosome dynamics, we found that the most informative movies contained 20–30 time-lapse images collected at 10-, 20-, and 30-s intervals at a single *Z*-plane. These image numbers and imaging intervals guaranteed no photobleaching or tissue damage, which could occur with more numerous or frequent exposures. Movies covering longer time spans, for example, containing 20–30 images collected at 1–2-min intervals, are valuable sources of information on longer term chromosome dynamics. However, we often found these movies difficult to analyze as anthers may move, even if slightly, in the microscope field of view after several minutes of imaging. If this happens, post-image analysis may still yield valuable information from these movies, particularly if the objects migrate at the end of the capture sequence.

We also make time-lapse image stacks with objects imaged at several *Z*-sections at every time point, usually 2–5 μ apart, to create 3D, multichannel, time-lapse movies. These movies offer wealth of information for understanding of the three-dimensionality of chromosome dynamics. They are, however, more difficult to analyze than the single *Z*-section movies.

It may be necessary to test several different combinations of image numbers, image capture intervals, *Z*-section numbers, etc., for every different imaging goal, MPE workstation type, meiosis stage, species, etc.

3.5. Image analysis with ImageJ

We exclusively use ImageJ, a freeware imaging analysis package, for processing and analyzing live imaging movies. All files are imported to ImageJ as grayscale image stacks. In multiwavelength imaging, each image is a composite of several wavelength channels, which can be false-colored.

3.5.1. Improving image quality

Prior to any analyses, images are despeckled to improve the signal-to-noise ratio. To improve the ability to identify cellular objects in the images, the Find Edges algorithm of ImageJ (available under the process menu) can also be used. This algorithm analyses the intensity (brightness) of adjacent pixels to define boundaries of objects, which are placed where the pixel intensity values change. We use this feature to delineate the nuclear boundaries and identify the position of the nuclear envelope, utilizing the relatively small difference in brightness between the cytoplasm and the nucleoplasm.

The Image Stabilizer plugin (Kang Li and Steven Kang) can be used to stabilize images of objects exhibiting jittery movements due to stage vibrations, cellular motions, or for any other reasons. It can also be used to electronically immobilize objects that move laterally across the field of view. Using this plugin, the object is "pinned" down in one place. Doing this allows for analysis of smaller objects moving inside larger objects that also move, for example, analysis of fine movements of individual chromosome segments inside nuclei that exhibit rotational movements of the whole chromatin. Relative velocities of the small chromosome segments can be determined without confounding them with the movement of the entire nucleus.

3.5.2. Generating flat projections

For files containing multi-*Z*-image stacks, flat projections can be generated in ImageJ using a built-in algorithm *Z* Project and a plugin, Grouped_Z-Project (Charles Holly, Holly Mountain Software). Both algorithms generate flat projections from several *Z*-sections in still 3D images or in 3D movies. Flat *Z*-projections are helpful in simplifying 3D images and can be generated based on the average intensity, the maximum intensity, or by a sum of slices.

3.5.3. Measuring object properties

To obtain basic measurements of cellular structures (such as nuclei, nucleoli, or the whole chromatin mass in the nucleus) in still images or in single frames of time-lapse movies, we use the drawing tools and the Region-of-Interest

(ROI) manager of ImageJ. The drawing tools can also be used to select and straighten curved chromosomes to measure their length.

To track and analyze movements of small, single-point objects moving in time in time-lapse movies, we use two-particle tracking plugins that

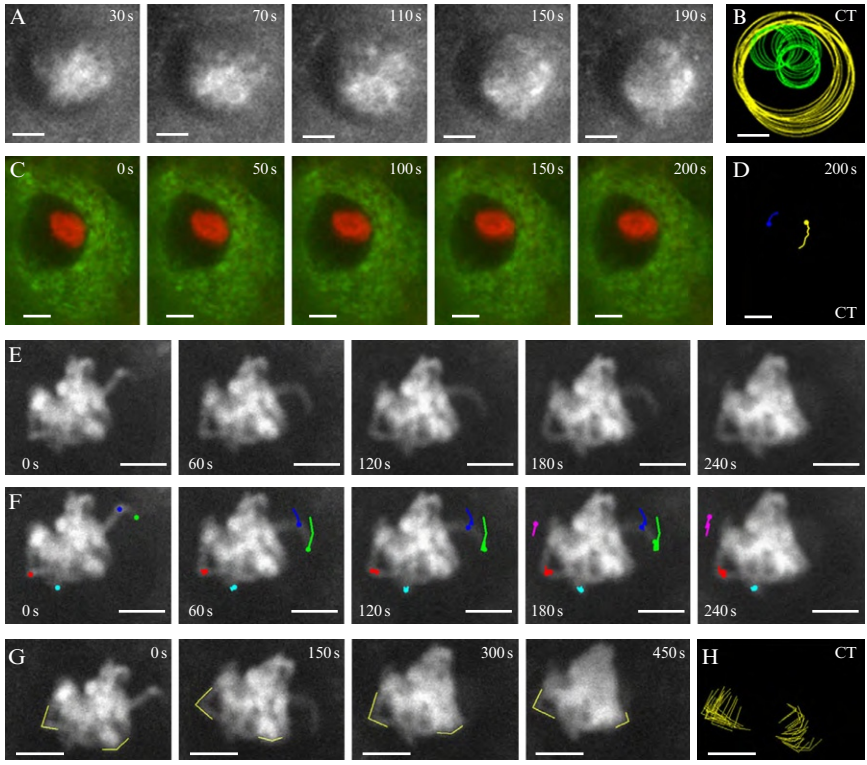

Figure 7.4 Patterns of chromosome movements during meiotic prophase I in maize. (A) A zygotene nucleus exhibiting rotational motions. (B) Cumulative tracks of the nuclear envelope (yellow) and nucleolus (green) in the nucleus in A after 190 s. (C) A zygotene nucleus showing sliding rotation of the entire chromatin (red) along the nuclear envelope. Green = cytoplasm stained with Rhodamine 123. (D) Cumulative tracks of two anonymous chromosome marks located at the nuclear periphery in the nucleus shown in C after 200 s. (E) Rotational movements of the entire chromatin in a pachytene nucleus. (F) The nucleus shown in E overlaid with trajectories of chromosome marks shown every 60 s for 240 s. Green and blue mark the chromosome end and an interstitial knob, respectively, of a chromosome arm, which exhibits long-distance sweeping movements. Red = a chromosome loop whose both ends are embedded in the chromatin mass. Cyan = a stationary chromosome region on the periphery of the chromatin mass. Magenta = a free, fast-moving chromosome end. (G) The nucleus shown in E with yellow lines marking chromatin mass edges. (H) Cumulative tracks from G after 570 s but without chromatin shown. Bars = 5 μm. Adapted from Sheehan and Pawlowski (2009).

essentially perform the same task: MTrackJ (Erik Meijering) and Particle Tracker (Sbalzarini and Koumoutsakos, 2005). MTrackJ is easier to use and provides the ability to produce publication-quality outputs as it offers more editing options and has a more user-friendly interface. To track an object, one must manually select it in each time frame. Several objects can be tracked independently in parallel by using differently colored tracks. To do this, one must first track one object and then do the same for each additional object. The object tracks can be saved as separate movies or can be overlaid over the objects in the originals movies (Fig. 7.4). Still images with cumulative tracks can also be generated. Statistics on velocity and movement directionality of the objects moving through time can also be generated.

To trace movements of larger objects, for example, movements of the entire chromatin mass in the nucleus or shape changes of the nuclear envelope, we utilize the segmented line feature. The object is delineated in each time frame and each of the object outlines is saved in the ROI manager. Finally, a time-lapse movie of the outlines is generated, which can be saved separately or overlaid over the originals movie (Fig. 7.4).

ACKNOWLEDGMENTS

The research relevant to this chapter was supported by a USDA-NRI postdoctoral fellowship to M. J. S. and a USDA-AFRI grant to W. P. P.

REFERENCES

Baluska, F., Jasik, J., Edelmann, H. G., Salajova, T., and Volkmann, D. (2001). Latrunculin B-induced plant dwarfism: Plant cell elongation is F-actin-dependent. *Dev. Biol.* **231,** 113–124.

Bass, H. W., Marshall, W. F., Sedat, J. W., Agard, D. A., and Cande, W. Z. (1997). Telomeres cluster de novo before the initiation of synapsis: A three-dimensional spatial analysis of telomere positions before and during meiotic prophase. *J. Cell Biol.* **137,** 5–18.

Baudrimont, A., Penkner, A., Woglar, A., Machacek, T., Wegrostek, C., Gloggnitzer, J., Fridkin, A., Klein, F., Gruenbaum, Y., Pasierbek, P., and Jantsch, V. (2010). Leptotene/zygotene chromosome movement via the SUN/KASH protein bridge in Caenorhabditis elegans. *PLoS Genet.* **6,** e1001219.

Chan, A., and Cande, W. Z. (2000). Maize meiocytes in culture. *Plant Cell Tissue Organ Culture* **60,** 187–195.

Chen, T., Teng, N., Wu, X., Wang, Y., Tang, W., Samaj, J., Baluska, F., and Lin, J. (2007). Disruption of actin filaments by latrunculin B affects cell wall construction in Picea meyeri pollen tube by disturbing vesicle trafficking. *Plant Cell Physiol.* **48,** 19–30.

Chikashige, Y., Ding, D.-Q., Funabiki, H., Haraguchi, T., Mashiko, S., Yanagida, M., and Hiraoka, Y. (1994). Telomere-led premeiotic chromosome movement in fission yeast. *Science* **264,** 270–273.

Conrad, M. N., Lee, C. Y., Chao, G., Shinohara, M., Kosaka, H., Shinohara, A., Conchello, J. A., and Dresser, M. E. (2008). Rapid telomere movement in meiotic prophase is promoted by *NDJ1*, *MPS3*, and *CSM4* and is modulated by recombination. *Cell* **133,** 1175–1187.

Cowan, C. R., and Cande, W. Z. (2002). Meiotic telomere clustering is inhibited by colchicine but does not require cytoplasmic microtubules. *J. Cell Sci.* **115,** 3747–3756.

Cowan, C. R., Carlton, P. M., and Cande, W. Z. (2001). The polar arrangement of telomeres in interphase and meiosis. Rabl organization and the bouquet. *Plant Physiol.* **125,** 532–538.

DeBolt, S., Gutierrez, R., Ehrhardt, D. W., Melo, C. V., Ross, L., Cutler, S. R., Somerville, C., and Bonetta, D. (2007). Morlin, an inhibitor of cortical microtubule dynamics and cellulose synthase movement. *Proc. Natl. Acad. Sci. USA* **104,** 5854–5859.

Denk, W., Strickler, J. H., and Webb, W. W. (1990). Two-photon laser scanning fluorescence microscopy. *Science* **248,** 73–76.

Emaus, R. K., Grunwald, R., and Lemasters, J. J. (1986). Rhodamine 123 as a probe of transmembrane potential in isolated rat-liver mitochondria: Spectral and metabolic properties. *Biochim. Biophys. Acta.* **850,** 436–448.

Feijo, J. A., and Cox, G. (2001). Visualization of meiotic events in intact living anthers by means of two-photon microscopy. *Micron* **32,** 679–684.

Gibbon, B. C., Kovar, D. R., and Staiger, C. J. (1999). Latrunculin B has different effects on pollen germination and tube growth. *Plant Cell* **11,** 2349–2363.

Golubovskaya, I. N., Harper, L. C., Pawlowski, W. P., Schichnes, D., and Cande, W. Z. (2002). The *pam1* gene is required for meiotic bouquet formation and efficient homologous synapsis in maize (*Zea mays*, L.). *Genetics* **162,** 1979–1993.

Harper, L., Golubovskaya, I., and Cande, W. Z. (2004). A bouquet of chromosomes. *J. Cell Sci.* **117,** 4025–4032.

Heslop-Harrison, J. (1966). Cytoplasmic connexions between angiosperm meiocytes. *Ann. Bot.* **30,** 221–230.

Hsu, S. Y., Huang, Y. C., and Peterson, P. A. (1988). Development pattern of microspores in *Zea mays* L. The maturation of upper and lower florets of spikelets among an assortment of genotypes. *Maydica* **33,** 77–98.

Johnson, L. V., Walsh, M. L., and Chen, L. B. (1980). Localization of mitochondria in living cells with rhodamine 123. *Proc. Natl. Acad. Sci. USA* **77,** 990–994.

Keij, J. F., Bell-Prince, C., and Steinkamp, J. A. (2000). Staining of mitochondrial membranes with 10-nonyl acridine orange, MitoFluor Green, and MitoTracker Green is affected by mitochondrial membrane potential altering drugs. *Cytometry* **39,** 203–210.

Koszul, R., Kim, K. P., Prentiss, M., Kleckner, N., and Kameoka, S. (2008). Meiotic chromosomes move by linkage to dynamic actin cables with transduction of force through the nuclear envelope. *Cell* **133,** 1188–1201.

Liu, Z., Bushnell, W. R., and Brambl, R. (1987). Pontentiometric cyanine dyes are sensitive probes for mitochondria in intact plant cells: Kinetin enhances mitochondrial fluorescence. *Plant Physiol.* **84,** 1385–1390.

Miller, A. L., and Gow, N. A. (1989). Correlation between root-generated ionic currents, pH, fusicoccin, indoleacetic acid, and growth of the primary root of *Zea mays*. *Plant Physiol.* **89,** 1198–1206.

Page, S. L., and Hawley, R. S. (2004). The genetics and molecular biology of the synaptonemal complex. *Annu. Rev. Cell Dev. Biol.* **20,** 525–558.

Paleček, J., and Hašek, J. (1984). Visualization of dimethyl sulphoxide-stabilized tubulin containing structures by fluorescence staining with monoclonal anti-tubulin antibodies. *Histochem. J.* **16,** 354–356.

Sbalzarini, I. F., and Koumoutsakos, P. (2005). Feature point tracking and trajectory analysis for video imaging in cell biology. *J. Struct. Biol.* **151,** 182–195.

Scherthan, H. (2007). Telomere attachment and clustering during meiosis. *Cell. Mol. Life Sci.* **64,** 117–124.

Scherthan, H., Wang, H., Adelfalk, C., White, E. J., Cowan, C., Cande, W. Z., and Kaback, D. B. (2007). Chromosome mobility during meiotic prophase in Saccharomyces cerevisiae. *Proc. Natl. Acad. Sci. USA* **104,** 16934–16939.

Sheehan, M. J., and Pawlowski, W. P. (2009). Live imaging of rapid chromosome movements in meiotic prophase I in maize. *Proc. Natl. Acad. Sci. USA* **106,** 20989–20994.

Trelles-Sticken, E., Adelfalk, C., Loidl, J., and Scherthan, H. (2005). Meiotic telomere clustering requires actin for its formation and cohesin for its resolution. *J. Cell Biol.* **170,** 213–223.

Williams, R. M., Zipfel, W. R., and Webb, W. W. (2001). Multiphoton microscopy in biological research. *Curr. Opin. Chem. Biol.* **5,** 603–608.

Xu, C.-H., Huang, S.-J., and Yuan, M. (2005). Dimethyl sulfoxide is feasible for plant tubulin assembly *in vitro*: A comprehensive analysis. *J. Integr. Plant Biol.* **47,** 457–466.

Yu, H.-G., Hiatt, E. N., Chan, A., Sweeney, M., and Dawe, R. K. (1997). Neocentromere-mediated chromosome movement in maize. *J. Cell Biol.* **139,** 831–840.

Zickler, D., and Kleckner, N. (1999). Meiotic chromosomes: Integrating structure and function. *Ann. Rev. Genet.* **33,** 603–754.